ELSEVIER

Polymer 41 (2000) 629–637

polymer

Effect of film thickness on the changes in gas permeability of a glassy polyarylate due to physical aging
Part I. Experimental observations

M.S. McCaig, D.R. Paul*

Department of Chemical Engineering and Center for Polymer Research, University of Texas at Austin, Austin, TX 78712, USA

Received 20 November 1998; accepted 23 February 1999

Abstract

The effects of thickness (0.25–33 μm) and aging time on the gas permeation properties of films formed from a glassy polyarylate made from bisphenol-A benzophenone dicarboxylic acid were examined. Evidence is presented which shows that physical aging is responsible for a significant decrease in gas permeability with time following quenching the polymer from above its glass transition temperature; the rate of change is greater for the thinner films. Two methods of determining accurate film thicknesses were used to obtain absolute permeability coefficients. The importance of the permeation protocol on the aging rate was examined, and a reversal of the aging process was demonstrated by annealing the aged film above the T_g. These results indicate that physical aging occurs by two distinct simultaneous mechanisms: one which is thickness dependent and another that is not. © 1999 Elsevier Science Ltd. All rights reserved.

Keywords: Glassy polyarylate; Physical aging; Film thickness

1. Introduction

Industrial gas separation processes utilize very thin membranes to achieve high productivity; however, much of the research on screening or developing new materials for these processes has been performed on thick films. Recent studies have shown that the gas flux or permeance of very thin glassy polymeric membranes can dramatically decrease over relatively short time scales [1–3]. It has been suggested that this is a result of a physical aging process that is accelerated in very thin films.

Physical aging in amorphous polymers is a consequence of the non-equilibrium nature of the glassy state and consists of a continual evolution towards equilibrium; although, the rate is usually exceedingly slow except just below the glass transition temperature, T_g [4–9]. This leads to changes in polymer properties, e.g. a decrease in enthalpy, creep rate and toughness and an increase in density, storage modulus and yield stress, etc [10,11]. These time-dependent changes are related to volume relaxation, which causes a decrease in segmental mobility of the polymer chains [7,12,13]. The effect of sample size on the rate of volume relaxation has been debated over the years. Braun and Kovacs suggested that the rate of physical aging is independent of thickness based on some limited observations [14,15], but Koros et al. [1–3] have documented a substantial flux decay, which can be interpreted as a loss in free volume, over time in thin films that is not observed in thick films. In 1943, Alfrey et al. [16] proposed diffusion of free volume or “holes” as a means of volume relaxation in glassy polymers which would, at least in principle, explain such size effects; however, Kauzmann [17] objected to the general notion of diffusion of free volume which led Hirai and Eyring [18] to develop a model for an alternative mechanism. The literature continues to invoke free volume diffusion as a mechanism, at least qualitatively, for volume relaxation [1–3,7,8,11,13,19–22]. For example, Curro et al. [19] proposed a dual mechanism for free volume reduction in which “lattice contraction”, similar to the concept proposed by Hirai and Eyring, and free volume diffusion occur simultaneously.

In this article, the effects of physical aging on the gas permeation properties of bisphenol-A benzophenone-dicarboxylic acid (BPA-BnzDCA) films are examined. We are able to report absolute permeability coefficients, P, instead of the observed permeance, P/ℓ, in contrast to most other studies on very thin films, because accurate values of the film thickness, ℓ, were measured using scanning electron microscopy and profilometry techniques. The structure and physical properties of BPA-BnzDCA are shown in Table 1

---

* Corresponding author. Tel.: +1-512-471-5392; fax: +1-512-471-0542.
E-mail address: paul@che.utexas.edu (D.R. Paul)

PII: S0032-3861(99)00172-X

Table 1
Polymer structure and physical properties

Structure	Polymer abbreviation	T_g (°C)	Density (g/cm^3)	FFV[a]
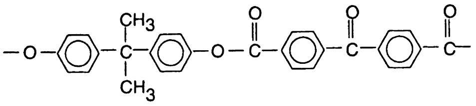	BPA-BnzDCA	194	1.231	0.149

[a] Calculated from experimental specific volume and an estimate of occupied volume using the method of Bondi23.

[23]. BPA-BnzDCA was chosen because the diacid structural segment will be used in future work to study the effect of UV crosslinking on the permeation behavior of thin polyarylate films. Oxygen permeability of thin films can be measured accurately and is a sensitive indicator of small changes in free volume; this proves to be a very effective way of monitoring the process of physical aging. The effects of film thickness, feed pressure and annealing temperature are examined here to gain insights about the mechanism of physical aging. The effect of film thickness on the rate of permeability change was studied in great detail because this provides a powerful way to explore the notion of free volume diffusion as a mechanism of physical aging; the time, t, response of a diffusion controlled phenomenon for films of different thicknesses should scale as t/ℓ^2. Reversal of the aging process by re-heating the membrane above T_g is also demonstrated. This study presents the experimental results in a phenomenological manner, while the second one in this series attempts to quantitatively model these results in terms of processes identified in the present study.

2. Materials and methods

BPA-BnzDCA was synthesized (see Table 2 for starting monomers) by an interfacial polymerization method described by Morgan [24]. The BPA was used as received from Aldrich Chemical. The BnzDCA, graciously donated by Nihon Nohyaku, was refluxed with excess thionyl chloride and purified by vacuum distillation to yield the diacid chloride [25]. The polymer was reprecipitated twice from chloroform into ethanol and then vacuum dried to remove residual solvent.

Table 2
Monomer sources and purification

Monomer	Source	Purification	Melting point (°C)
Bisphenol-A (BPA)	Aldrich	None	158–159
Benzophenone dicarboxylic acid (BnzDCA)	Nihon Nohyaku	None	[a]

[a] Decomposes at 260°C before melting.

The glass transition temperature was measured using a Perkin–Elmer DSC-7 differential scanning calorimeter at a heating rate of 20°C/min. The sample was scanned twice and the T_g evaluated at the onset of the transition in the second scan. The polymer appears to be amorphous due to its clarity and the absence of a crystalline melting point. The polymer density was measured in a density gradient column based on aqueous calcium nitrate solutions at 30°C.

All films were prepared by solution casting on silicon wafers inside metal casting rings. The solution concentration was adjusted to obtain film thicknesses ranging from 0.25 to 33 μm. The thick films ($\ell > 2.5$ μm) were removed from the wafer and vacuum dried at room temperature for 24 h and then at 150°C for 5 days according to the standard procedures established in this laboratory for film preparation prior to permeation testing. Thermogravimetric analysis (TGA) using a Perkin–Elmer TGA-7 was used to confirm the complete removal of solvent. The thin films ($\ell < 2.5$ μm) were floated off the casting surface with water and then lifted onto porous ceramic supports. To ensure solvent removal, the procedures established by Pfromm [1] were used; the thin films were allowed to air dry overnight, then dried at 100°C for 24 h and finally annealed at 230°C, which is well above the $T_g = 194$°C, for 2 h. This produced a very thin yet dense polymer layer supported by a porous ceramic layer; the polymer layer was not constrained by the support, as it could be removed by simply lifting it off the ceramic. Using separate methods of film preparation for the thin and thick films did not have a substantial effect on the permeation properties particularly as all the films were annealed at 230°C for 2 h prior to aging.

After annealing above the T_g at 230°C, the films were quickly removed from the vacuum oven, thereby “quenching” the polymer; this is assumed to be $t = 0$ for all aging considerations. The films used to evaluate the “bulk” permeation behavior were prepared following the standard protocol described above. A temperature probe encased in the middle of a 102 μm sample of BPA-BnzDCA was heated to 250°C, and then the polymer and probe were removed from the oven to simulate the slowest possible quench experienced by the samples in this study, where thicknesses ranged from 0.25 to 33 μm. The heat loss experienced by the bare probe was also measured and

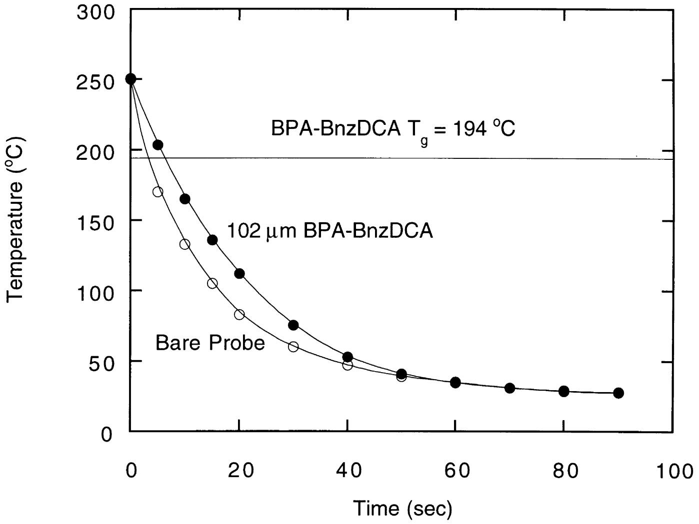

Fig. 1. Observed quench rate for a 102-μm sample of BPA-BnzDCA (●) and the bare temperature probe (○) following removal from a vacuum oven at 250°C.

plotted to show the maximum measurable quench rate by this technique. The minimum and maximum quench rates are shown in Fig. 1, and there is relatively small difference between them. The temperature in the thick film falls significantly below the T_g within 5 s of removal from the oven.

The film thickness was measured by a micrometer for values greater than 2.5 μm, while this technique is not as accurate as the SEM technique described subsequently, it does provide an adequate level of accuracy for reporting absolute permeability values. As mentioned, the SEM procedure was used for films thinner than 2.54 μm. Following completion of the permeation measurements, the composite membranes were cooled in liquid nitrogen and fractured to yield a polymer–ceramic cross-section; photomicrographs using a JEOL JSM-35c SEM microscope were then taken of an edge view of the polymer–ceramic composite membrane. The SEM technique compares a secondary electron image to a backscattered electron image during a single scan; the former shows both the polymer and ceramic, while in the latter only the ceramic support is visible due to its higher atomic mass. Fig. 2 shows an example of the image obtained by this technique; the right half of the scan is the secondary electron image which shows the polymer and ceramic, while the left half of the scan is the backscattered image where only the ceramic support is discernible. This provides a clear picture of the polymer film thickness and shows that the polymer does not invade the ceramic pores. The thickness of the polymer–ceramic membrane was measured with a micrometer prior to mounting the samples for SEM; this thickness was used in conjunction with lower magnification photos of the entire cross-section to verify the accuracy of the scale on the SEM photomicrograph. The validity of this method for obtaining accurate thicknesses was verified by performing profilometry on several of the films prior to their removal from the silicon substrate. It is important to obtain an accurate measurement of the film thickness, ℓ, so that the absolute permeability coefficient, P, can be calculated rather than simply reporting the observed permeance, P/ℓ, as is done in most studies of such thin films.

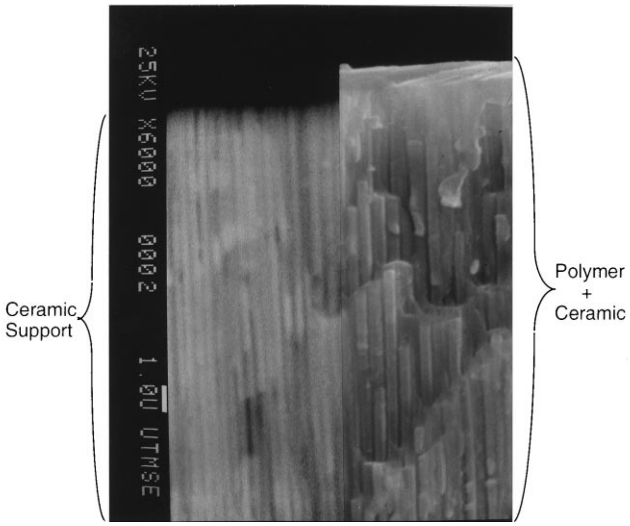

Fig. 2. Edge view of a polymer–ceramic composite film; the right half shows the polymer and ceramic while the left half shows only the ceramic.

The specific volume of BPA-BnzDCA was measured as a function of pressure in isothermal experiments on a Gnomix PVT apparatus. Fig. 3 shows the PVT behavior obtained from these experiments over a pressure range of 0–50 MPa for temperatures from 50 to 280°C.

Pure gas permeability coefficients were evaluated at 35°C and 2 atm for O_2 and N_2 using a standard pressure-rise type permeation cell following standard procedures employed in this laboratory [25]. Liquid nitrogen traps were used on all permeation equipment and vacuum ovens to eliminate possible pump oil contamination of the samples.

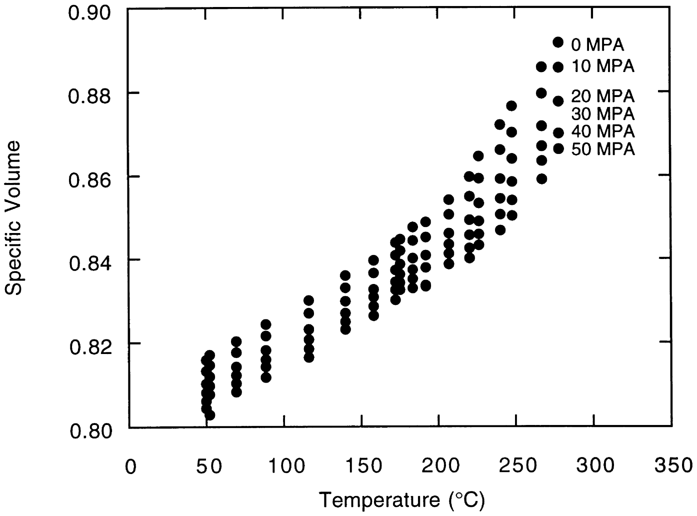

Fig. 3. PVT data for BPA-BnzDCA; specific volume is shown as a function of temperature for pressures ranging from 0 to 50 MPa.

3. Alternative explanations to physical aging

This investigation was initiated as a result of the observation of significant decreases in the absolute gas permeability as a function of time after preparation of thin polyarylate films intended for a study of the effect of UV crosslinking on separation performance. There is convincing evidence that these observations reflect a physical aging phenomenon; however, other alternatives were explored and eliminated as explanations for the data. The first was the possibility of contamination of the sample by vacuum pump oil as noted in other similar studies [26,27]. This seemed unlikely due to the precaution of using liquid nitrogen traps on the vacuum pumps; nevertheless, a bubble flow meter was used to measure the oxygen permeability of BPA-BnzDCA as a function of time which avoids all exposure of the system to vacuum pump oil. A number of measurements by this method gave essentially the same results as obtained using a standard permeation cell with a vacuum pump. Thus, contamination was eliminated as a cause of the observed permeability reduction.

To assert that the observed changes in permeability with time are a consequence of physical changes that occur in the glassy state, it seemed important to show that similar changes do not occur in rubbery polymers. For this demonstration, the oxygen permeability of a thin poly(dimethyl siloxane), silicone rubber, film spun on a ceramic support and heated to 100°C in a vacuum oven was measured for over 48 h. The permeability response of the 0.61 μm PDMS film is shown in Fig. 4 as a function of time. The oxygen permeability coefficients are all within 10% of the published value of 933 barrers [28] and do not show a reduction over time. Any deviation from the expected value can be attributed to experimental error inherent in measuring the

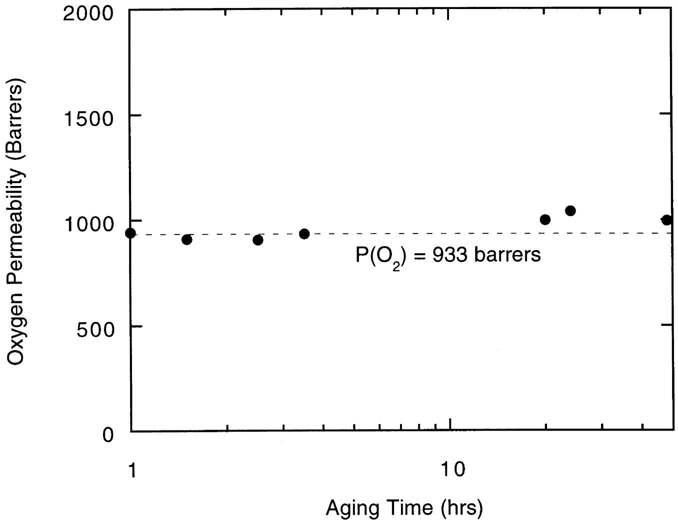

Fig. 4. Effect of aging time on the oxygen permeability coefficient of a 0.61-μm poly (dimethylsiloxane) film after quenching from 100°C. The dashed line is the oxygen permeability [28] value of 933 barrers.

Table 3
Bulk permeability and diffusivity coefficients for O_2/N_2 separation

Polymer	Temperature (°C)	P_{O_2}(Barrers)	α O_2/N_2	$D_{O_2}10^{-8}\left(\frac{cm^2}{s}\right)^a$	D_{O_2}/D_{N_2}
BPA-BnzDCA	35	1.58	4.81	3.4	3.06
	55	3.22	4.41	—	—

[a] Diffusion coefficient determined by time-lag method.

permeability coefficients for a thin membrane of a highly permeable material such as PDMS.

These results eliminate some possible causes that have been suggested for the time-dependent behavior shown next. The observations described here add justification for attributing the permeability change with time to physical aging; the thermal reversibility demonstrated later provides even stronger evidence.

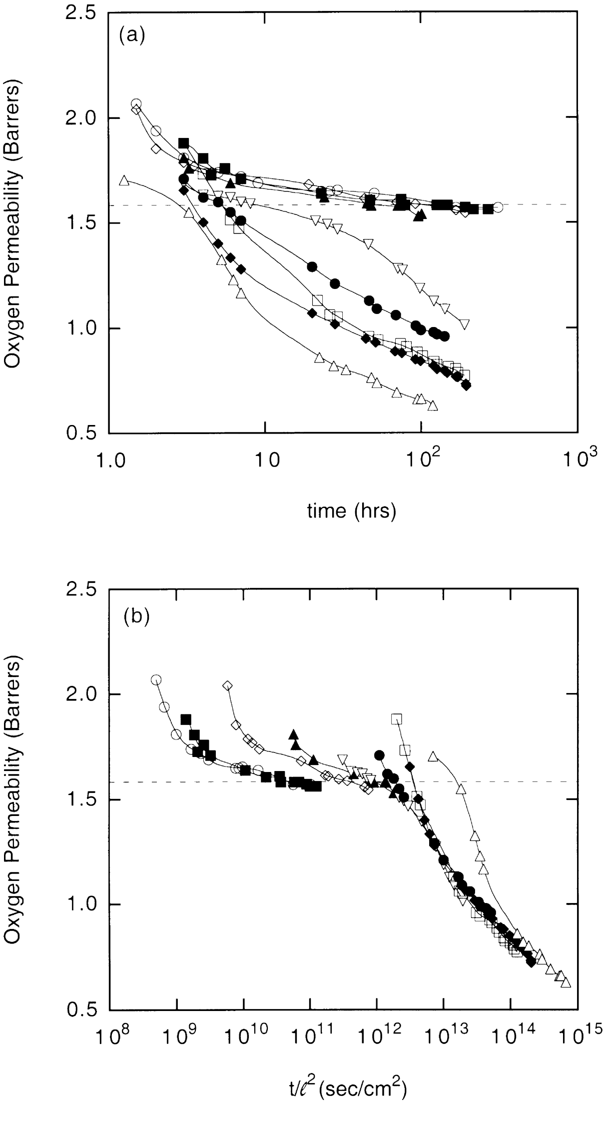

Fig. 5. Effect of aging time, t, (a) and normalized aging time, t/ℓ^2, (b) on the oxygen permeability coefficients for BPA-BnzDCA for films of the following thickness: (○) 33, (■) 28, (◇) 9.7, (▲) 4.4, (▽) 1.85, (●) 0.99, (□) 0.74, (◆) 0.58, and (△) 0.25 μm.

4. Results and discussion

4.1. Effect of film thickness on aging rate

To our knowledge, there are no prior reports on the synthesis or the properties of BPA-BnzDCA. In this study, the permeation properties were measured over a range of thicknesses (0.254–33 μm) for an extended period of time after preparation of the film. The "bulk" permeability and diffusivity values for O_2 and N_2 were measured for "thick" films at 35 and 55°C respectively, and 2 atm for comparison purposes with the permeation properties of "thin" films as a function of aging time. The bulk values are shown in Table 3 and on each aging figure as a horizontal dashed line that does not change with time. "Bulk" values are defined here as gas transport coefficients measured on very thick films ($\ell > 30$ μm) according to standard procedures established in this laboratory. The gas transport properties were measured at 35°C and 2 atm for O_2 and N_2 except where noted. Fig. 5(a) shows the oxygen permeability of BPA-BnzDCA films at 35°C as a function of time for a series of films with thicknesses ranging from 0.25 to 33 μm after quenching from above the T_g. It is interesting to note that all the absolute permeability coefficients begin above the "bulk" value of 1.58 barrers. For films ranging in thicknesses from 0.25 to 1.85 μm, the extent of permeability reduction appears to be a strong function of the thickness; the thinnest films exhibit the most rapid reduction in oxygen permeability. The aging exhibited by the thicker films (4.4–33 μm) is less dramatic and does not seem to be a function of thickness over the time scale investigated here. If the volume relaxation or physical aging process that is believed to be the cause of the observed time dependence of permeability occurs by "diffusion" of free volume to the film surface, as suggested earlier, then the response observed here should collapse to a single curve when plotted versus the combined variable t/ℓ^2. As seen in Fig. 5(b), the situation is more complex than this. The permeability reduction over the range of thicknesses is initially very rapid and does not scale as t/ℓ^2, but for longer times all the data eventually collapse onto a single "master" curve; thus, such plots do provide an informative way of representing the response.

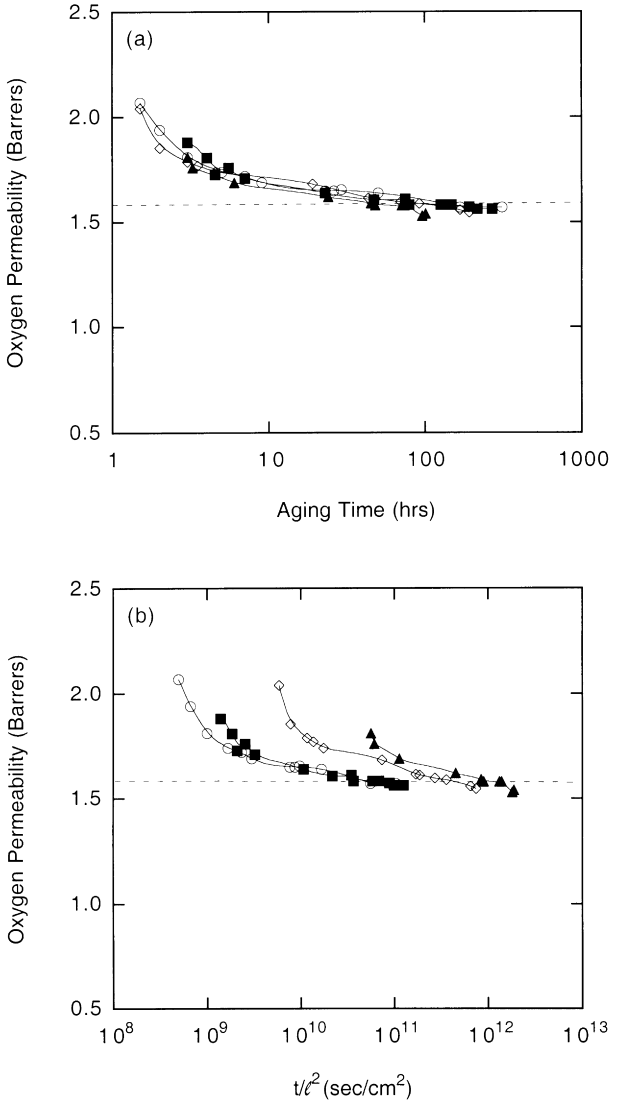

Fig. 6. Effect of aging time, t, (a) and normalized aging time, t/ℓ^2, (b) on the oxygen permeability coefficients for thick BPA-BnzDCA films ($\ell > 2.5$ μm): (○) 33, (■) 28, (◇) 9.7, and (▲) 4.4 μm.

Fig. 6(a) shows that the majority of permeability reduction for thick films ($\ell \geq 4.4$ μm) takes place during the first 10 h of aging and then slows significantly as the O_2 permeability values approach the bulk value. All the thick films aged at a similar rate, i.e. there does not seem to be any dependence on thickness. Fig. 6(b) clearly illustrates the non-scaling nature of the permeability reduction observed initially. As shown in Fig. 7, the oxygen permeability of thin films ($\ell \geq 1.85$ μm) more nearly collapses onto a single curve as aging progresses and the slope of the curve appears to decrease as t/ℓ^2 gets larger. The initial aging of these thin films also exhibits some non-scaling behavior which is most clearly seen for the 0.25 μm film.

It is well known that for a series of similar polymers, a trade-off is observed between gas permeability and selectivity [29–37]. Robeson [38] has compared the selectivity versus permeability for an extensive database of different polymers and has proposed an "upper bound" trade-off relationship. Fig. 8 shows that as films age, the O_2/N_2 selectivity increases. Although the data are somewhat limited, some important observations can be made. The general trend is that selectivity increases with aging while permeability coefficients decrease which is consistent with commonly observed trade-off relationships. The O_2/N_2 selectivity values begin below the bulk value of 4.81 and increase to values higher than this with aging; Pfromm and Koros [1] and Rezac et al. [2,3] reported similar trends for very different polymers. The slopes of the initial increase in selectivity are similar and do not scale as t/ℓ^2, but as aging time increases, the curves begin to approach each other and the slope decreases.

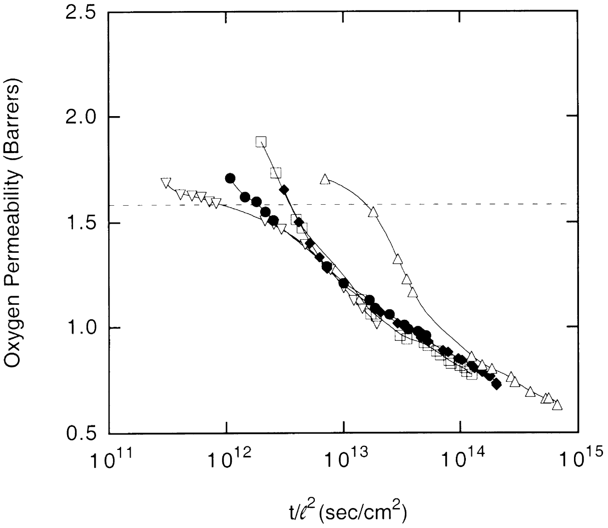

Fig. 7. Effect of normalized aging time (t/ℓ^2) on the oxygen permeability coefficients for thin BPA-BnzDCA films ($\ell < 2.5$ μm): (▽) 1.85, (●) 0.99, (□) 0.74, (◆) 0.58, and (△) 0.25 μm.

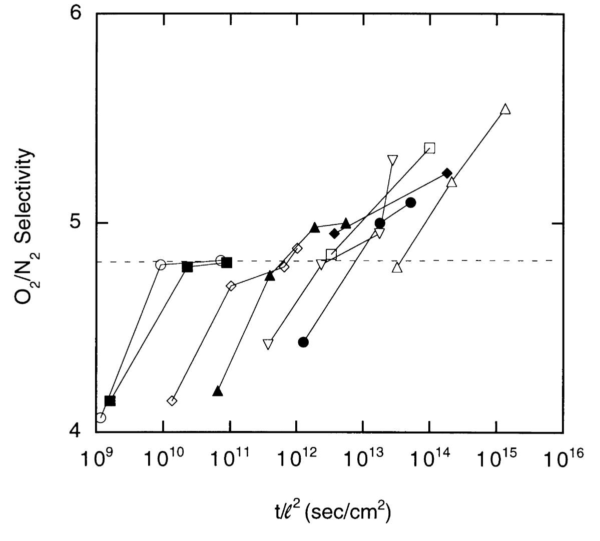

Fig. 8. Effect of normalized aging time (t/ℓ^2) on the O_2/N_2 selectivity coefficients for BPA-BnzDCA as a function of film thickness: (○) 33, (■) 28, (◇) 9.7, (▲) 4.4, (▽) 1.58, (●) 0.99, (□) 0.74, (◆) 0.58, and (△)

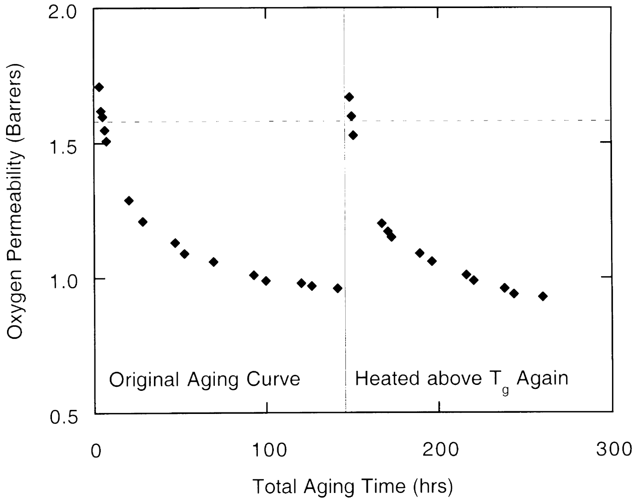

Fig. 9. Demonstration of the reversal of the effects of aging on the oxygen permeability coefficients by heating above the T_g again. The vertical line marks the time in the aging experiment when the membrane was re-heated above the T_g.

4.2. Proof of thermal reversibility

Studies of other properties have shown that the consequences of physical aging can be reversed by simply heating the sample above T_g again [7,10]; this should also be true for the observed changes in permeability. To demonstrate this, the permeability of a 0.99-μm film was monitored for 141 h. The sample was then removed from the permeation cell and heated to 230°C for 2 h after which it was "quenched" using the previously described procedures; permeation measurements were again made as a function of aging time. Both the original aging curve and that following the re-heat are shown in Fig. 9. The original loss in oxygen permeability in the first aging cycle is recovered after heating above T_g; the aging response in the second cycle is quite similar to that observed in the first. This demonstration of reversibility is further strong evidence that physical aging or volume relaxation of the polymer glass is the cause of the permeability losses and selectivity gains shown in Figs. 5–8.

4.3. Effects of aging temperature and gas pressure

The details of how the gas permeation rates are measured could influence the observed aging [39,40]. Fig. 10 shows the results from an aging experiment where the gas feed pressure and the vacuum cycle during measurements were varied from the standard protocol. Following each "standard" permeation measurement, a vacuum is applied for both upstream and downstream to degas the membrane. As the time for a permeation measurement is short compared to the aging time, the majority of the aging takes place under vacuum. For oxygen, the typical gas feed pressure is 2 atm during a permeation measurement. These standard procedures were used to measure oxygen permeability on a 0.74-μm film and the aging results are plotted as open circles in Fig. 10. As an alternative, a 0.58-μm film was aged under a constant upstream pressure of 5 atm of oxygen (vacuum downstream), without degassing between permeation measurements (see the closed triangles in Fig. 10). The results from this test are essentially identical to results obtained using the standard protocol; thus, over this range the measurement protocol does not influence the aging response.

Polymer segmental mobility is obviously an important factor that governs the rate of physical aging. All the permeation responses shown to this point were measured at 35°C; use of a higher temperature should increase the aging rate due to an associated increase in chain mobility. Fig. 11 compares the oxygen permeation responses at 55 and 35°C for two films of nearly identical thickness, 0.58

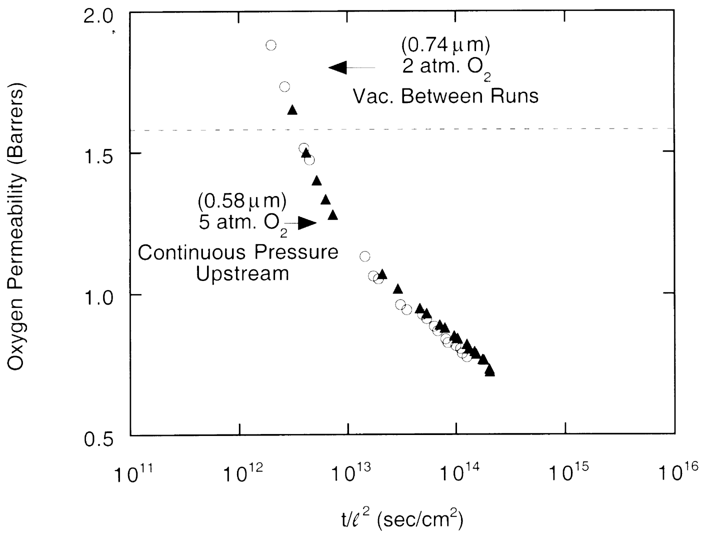

Fig. 10. Effect of deviation from the standard permeation protocol on the oxygen permeability coefficients: (○) standard protocol (2 atm O_2 pressure and degassing between measurements), (▲) alternate protocol (constant upstream O_2 pressure of 5 atm).

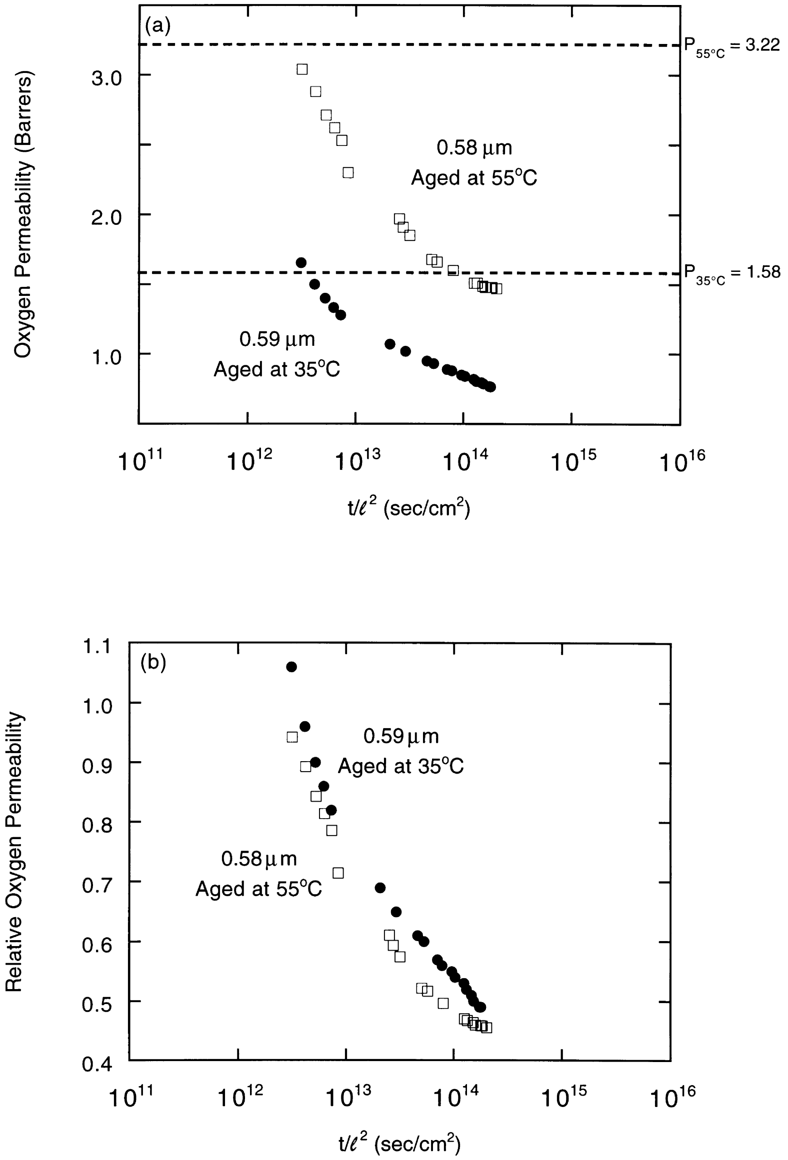

Fig. 11. Effect of aging temperature on the absolute oxygen permeability (a) and relative oxygen permeability (b) for films of nearly identical thickness: (□) 0.58 mm aged at 55°C, (●) 0.59 mm aged at 35°C. The dashed horizontal lines are the bulk values measured at 55°C (upper line) and 35°C (lower line).

and 0.59 μm. In Fig. 11(a), the absolute oxygen permeability coefficients are shown as a function of time. The permeability to O_2 at 55°C is higher than that at 35°C, as expected. To make a more direct comparison, the permeability coefficients for the aged samples were normalized by their corresponding bulk permeability value at the temperature of measurement (Table 3) with the results shown in Fig. 11(b). The curves are similar, but at the same aging time the relative permeability coefficients are always lower at 55°C than at 35°C; the 55°C data seem to be approaching some minimum value more rapidly than those at 35°C. A more complete study of the effects of temperature on aging response would no doubt be quite informative but was beyond the scope of the current work.

5. Summary and conclusions

The effects of film thickness on the physical aging of glassy BPA-BnzDCA was studied by monitoring the time evolution of the permeability to gases, primarily O_2. The permeability decreases and selectivity increases with aging time. These changes are believed to be the result of a decrease in polymer free volume which appears to occur by two distinct mechanisms. For thick films ($\ell > 2.5$ μm), the observed permeability loss is relatively small and appeared to approach the bulk value after 10 h of aging time following a quench from above the T_g; the rate of permeability loss appears to be independent of thickness. Conversely, the observed loss in absolute oxygen permeability for the thin films ($\ell < 2.5$ μm) was much larger than that in the thick films and the rate was strongly dependent on film thickness which can be explained by assuming that free volume is lost by diffusion to the film surface. The aging process was shown to be reversed by heating above the T_g. The effects of aging temperature and details of the permeation protocol were examined briefly.

The second part of this series [41] attempts to quantitatively describe the observed changes in the permeation properties of BPA-BnzDCA films as a function of aging time and film thickness in terms of a mathematical model that envisions both mechanisms mentioned earlier to occur simultaneously.

Acknowledgements

This research was supported by the Department of Energy, Basic Sciences Program, under Grant DE-FG03-95ER 14538 and the Separations Research Program at the University of Texas at Austin. Special thanks are extended to Nihon Nohyaku Co. for supplying the benzophenone dicarboxylic acid and Dr William J. Koros and Dr Peter H. Pfromm for their insights about the aging process. Special thanks are also extended to Dr Michael Schmerling for his essential help with the SEM techniques used here.

References

[1] Pfromm PH, Koros WJ. Polymer 1995;36:2379.
[2] Rezac ME, Pfromm PH, Costello LM, Koros WJ. Ind Chem Engng Res 1993;32:1921.
[3] Rezac ME. Ind Chem Engng Res 1995;34:3170.
[4] Heater, K.J. PhD Dissertation, Duke University, 1991.
[5] Chan AH, Paul DR. J Appl Polym Sci 1980;25:971.
[6] Chan AH, Paul DR. Polym Sci Engng 1980;20:87.
[7] Chang GW, Jamieson AM, Yu Z, McGervey JD. J Appl Polym Sci 1997;63:483.
[8] Muzeau E, Vigier G, Vasoille R. J Non-cryst Solids 1994;172–174:575.
[9] Sandreczki T, Hong X, Jean Y. Macromolecules 1995;29:4015.
[10] Royal JS, Torkelson JM. Macromolecules 1993;26:5331.
[11] Hill AJ, Heater KJ, Agrawal CM. J Polym Sci: Part B: Polym Phys 1990; 28:387.
[12] McHerron DC, Wilkes GL. Polymer 1993;34:915.
[13] Bartos J, Muller J, Wendorff JH. Polymer 1990;31:1678.
[14] Braun G, Kovacs AJ. J Phys Chem Glasses 1958;4:152.
[15] Kovacs AJ. J Polym Sci 1958;30:131.
[16] Alfrey T, Goldfinger G, Mark H. J Appl Phys 1943;14:700.
[17] Kauzmann W. Chem Rev 1948;43:219.
[18] Hirai N, Eyring H. J Appl Phys 1958;29:810.
[19] Curro JG, Lagasse RR, Simha R. Macromolecules 1982;15:1621.
[20] Hooker JC, Torkelson JM. Polym Prepr Am Chem Soc Div Polym Chem 1995;36:390.
[21] Bogdanova LM, Ponomareva TI, Irzhak VI, Rozenberg BA. Polym Sci, USSR 1984;26:1566.
[22] Chow TS. Macromolecules 1984;17:2336.
[23] Bondi A. Physical properties of molecular crystals, liquids and glasses. New York: Wiley, 1968.
[24] Morgan PW. Macromolecules 1970;3:536.
[25] Pixton, M. PhD Dissertation, University of Texas, 1995.
[26] Nagai K, Nakagawa T. J Memb Sci 1995;105:261.
[27] Morisato A, He Z, Pinnau I. Polym Prepr Am Chem Soc Div Polym Chem 1997;38:254.
[28] Ho WS, Sirkar KK. Membrane handbook. New York: Van Nostrand Reinhold, 1992.
[29] Aitken CL, Koros WJ, Paul DR. Macromolecules 1992;25:3425.
[30] Aitken CL, Koros WJ, Paul DR. Macromolecules 1992;25:3651.
[31] Kim TH, Koros WJ, Paul DR. J Memb Sci 1988;37:45.
[32] McHattie JS, Koros WJ, Paul DR. Polymer 1991;32:840.
[33] McHattie JS, Koros WJ, Paul DR. Polymer 1991;32:2618.
[34] McHattie JS, Koros WJ, Paul DR. Polymer 1992;33:1701.
[35] Pixton MR, Paul DR. J Polym Sci: Part B: Polym Phys 1995;33:1353.
[36] Pixton MR, Paul DR. J Polym Sci: Part B: Polym Phys 1995;33:1135.
[37] Pixton MR, Paul DR. Macromolecules 1995;28:8277.
[38] Robeson LM. J Memb Sci 1991;62:165.
[39] Enscore DJ, Hopfenberg HB, Stannett VT, Berens AR. Polymer 1977;18:1105.
[40] Pinnau I, Casillas CG, Morisato A, Freeman BD. J Poly Sci: Part B: Polym Phys 1997;35:1483.
[41] McCaig MS, Paul DR. Polymer 2000;41:639.